

Simulation studies of the Proportional Resonant controller

Abstract. Paper shows Proportional Resonant controller concept, that can track sinusoidal signals. Results of simulation studies of the 1 phase converter controlled by P+R controller, that connects DC voltage supply (e.g. renewable energy source) with low voltage network, were shown, for typical operational state of the power grid.

Streszczenie. W artykule przedstawiono koncepcję regulatora proporcjonalno rezonansowego, który posiada zdolność śledzenia sygnałów sinusoidalnie zmiennych. Zaprezentowano wyniki badań symulacyjnych jednofazowego falownika sprzęgającego źródło napięcia stałego (np. odnawialne źródło energii) z linią niskiego napięcia, wyposażonego w regulator rezonansowy dla typowych stanów eksploatacyjnych (**Badania symulacyjne regulatora Proporcjonalno Rezonansowego**).

Keywords: P+R controller, renewable energy sources, one phase converter, simulation studies

Słowa kluczowe: regulator P+R, odnawialne źródła energii, falownik 1-fazowy, badania symulacyjne

Introduction

The use of P or PI controllers, in rotating with the grid frequency dq frame is a common practice in regulation (current control) for the three phase converters in renewable energy systems „on grid”. This method is developed and commonly used but it requires considerable amount of the equipment and software (filtration, elimination of fixed components in measuring signals, etc.). In the one phase, devices which are usually used are PI controllers with big gain and low integration time (in relation to basic waveform period), which operate on pre-filtered signals. The applied filtration limits the dynamics of such controllers. Because of that, new solutions are being sought that will allow to control one and three phase converters [1, 2].

The use of so-called Proportional-Resonant Controller (P+R) proposed by R. Teoderescu and his team [3] can be an alternative solution. It can be used in one and three phase systems, for converters which operates with fixed frequency of the output voltage e.g. grid tied converters. This controller is dedicated in principle for one phase systems [4, 5]. In the three phase devices, after transformation to two phase orthogonal $\alpha\beta$ stationary frame, two identical controllers which operates in both axis, can be used [6]. Such a solution allows to control reactive current of the power line. The P+R controller can track sinusoidal signals and has selective amplitude and frequency response.

In the literature, besides typical structure of the P+R controller, modified types of controller can be found. They allow to improve controller operation in grids with unstable voltage and frequency through different variants of the feedback loop and controller transmittance [7, 8, 9]. There are also solutions based on the combination of typical PI and P+R controllers, which operate in dq synchronous frame [10] and in $\alpha\beta$ stationary frame [11]. The P+R controller can operate with different types of converters e.g. matrix converters [12] and multilevel converters [13] because converter topology and its control algorithm has no effect on the regulation method but only on the control technique.

The presented research was performed using basic P+R controller transmittance, which was given in [3]. The Controller was a part of the converter control system that tied energy source with power grid. The aim of the presented stage of studies, was to determine the impact of operating states of the power system on the device with the P+R. Reactions to the following events have been checked

- load changes,
- fluctuations of amplitude and voltage phase,

- voltage distortion,
- when resonant frequency of the P+R controller is not tuned to voltage frequency.

Research stage presented in article, so with continuous control system, is necessary in terms of the digital implementation of the controller. Thanks to this, it is possible to fully evaluate the response of the system resulting from the principle of its operation in real network operation conditions without discretization influence, necessary for controller realization in uP or FPGA technology. Controller discretization, implementation in real device and conducting the experiment are the next steps of the research.

P+R controller concept

P+R controller operates directly on variable signals. The transmittance of a resonant part of this controller was given in [1,2,5]. After adding a proportional part, the transmittance has form (1).

$$(1) \quad G_{P+R} = K_P + K_i \frac{2\xi\omega s}{s^2 + 2\xi\omega s + \omega^2}$$

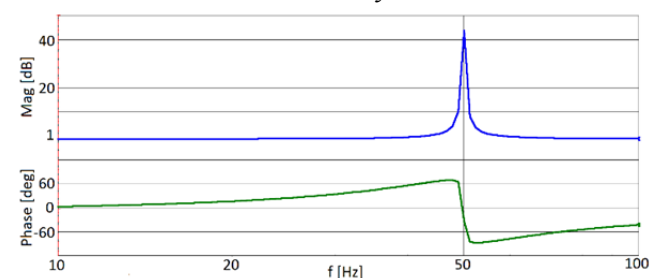


Fig.1. Amplitude and frequency characteristics for the P+R controller.

In the figure 1 amplitude and frequency characteristics were shown, for following parameters of controller described by (1): $K_P=1$, $K_i=100$, $\omega=100\pi$.

For the signals with frequency equal to resonant frequency gain is equal to K_P+K_i so, is much bigger than for signals with other frequencies. Further, signals with frequency not equal to resonant are phase shifted relative to input signal of the controller. [2]

P+R controller synthesis

For the simulation studies purpose, synthesis of P+R controller was made:

$$(2) \quad G_R = \frac{Y}{X} = \frac{s}{s^2 + 2\xi\omega s + \omega^2}$$

$$(3) \quad Ys^2 + 2Y\xi\omega s + Y\omega^2 = Xs$$

$$(4) \quad Y + \frac{Y2\xi\omega}{s} + Y\frac{\omega^2}{s^2} = \frac{X}{s}$$

$$(5) \quad Y = \frac{X}{s} - Y\frac{2\xi\omega}{s} - Y\frac{\omega^2}{s^2} = \frac{1}{s} \left[X - 2\xi\omega Y - \frac{\omega^2}{s} Y \right]$$

The controller with the structure based on (5) was shown on figure 2.

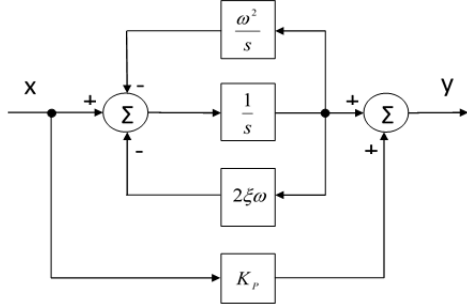


Fig.2. Structure of the P+R controller

The controller can be also implemented in the following way:

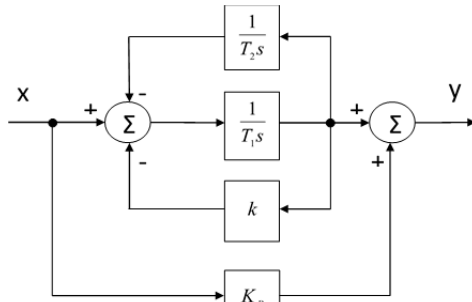


Fig.3. Implementation of the P+R controller

The controller with the structure from the figure 3 can be described by (6).

$$(6) \quad Y = \frac{1}{T_1 s} \left(X - \frac{1}{T_2 s} Y - kY \right)$$

Hence:

$$(7) \quad G_A = \frac{\frac{1}{T_1} s}{s^2 + \frac{k}{T_1} s + \frac{1}{T_1 T_2}} = K_i \frac{2\xi\omega s}{s^2 + 2\xi\omega s + \omega^2}$$

The equation (7) shows:

$$(8) \quad \omega = \frac{1}{\sqrt{T_1 T_2}} \quad \xi\omega = \frac{k}{2T_1} \quad K_i = \frac{1}{k}$$

From (8):

$$(9) \quad k = \frac{1}{K_i} T_1 = \frac{1}{2\xi\omega K_i} T_2 = \frac{1}{T_1 \omega^2}$$

For simplicity of transmittance $T_1 = T_2 = T$ can be assumed. Therefore:

$$(10) \quad G_A = \frac{\frac{1}{T} s}{s^2 + \frac{k}{T} s + \frac{1}{T^2}} = K_i \frac{2\xi\omega s}{s^2 + 2\xi\omega s + \omega^2}$$

Therefore, equation (10) coefficients are:

$$(11) \quad k = \frac{1}{K_i} \quad \omega = \frac{1}{T} \quad \xi = \frac{1}{2K_i}$$

According to the obtained structure from Fig. 3, such a regulator can be obtained from elements P and I.

Simulation studies of the one phase converter controlled by P+R controller

Simulation studies of the one phase converter controlled by P+R controller was made in IsSpice software. P+R controller was a part of the converter control system that connects energy source with electrical grid. In figure 4, there is a diagram of the system on which the tests were performed. Grid frequency was fixed (50 Hz). The phase voltage at the connection point was 230 V RMS. The voltage of the source, which was connected to the power grid by the inverter, was 400 V. It was assumed that the maximum power obtained from this source is 3 kW. The gain of a proportional K_P part was 1, while $K_I=100$. The amplitude of line current ($k_{I|sRef}$) set point was given. That signal is multiplied by scaled phase voltage (which is current waveform pattern) to obtain suitable line current waveform. The reference line current waveform which was obtained is compared with actual line current waveform (k_{I_s}). Gained error is inserted to P+R controller. To the output of the controller appropriately scaled phase voltage is added ($k_U U_s$). Its value is selected in such a way that the device from the beginning of the operation generates voltage equal to voltage at the connection point. In that case, controller generated signal is added to $k_U U_s$ in order to generate reference line current waveform to get reference waveform of the line current.

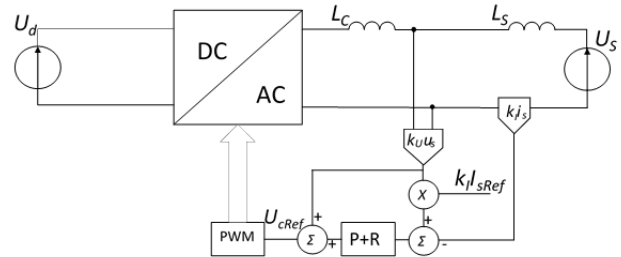


Fig.4. Studied device scheme

In the first stage of the research, system reaction to load changes was checked. Waveform in the figure 5 shows voltage at the point of connection do grid and line current, when the device starts with reference value of the line current amplitude equal to 18.3 A, and that corresponds to the maximum power (3 kW) possible to obtain from the energy source. Short after step change of reference waveform (t=25 ms), line current waveform obtained appropriate values.

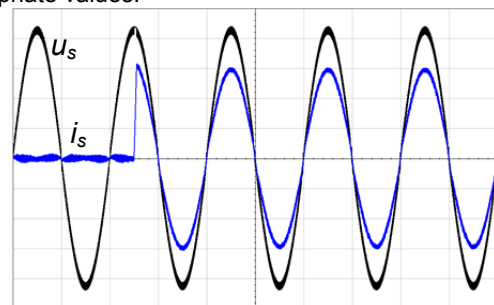


Fig.5. Waveforms of voltage u_s (75 V/div) and current i_s (6 A/div), during start for $t=0 \div 100$ ms (10 ms/div).

The reaction of the converter to load changes when the device operates was presented in the figure 6.

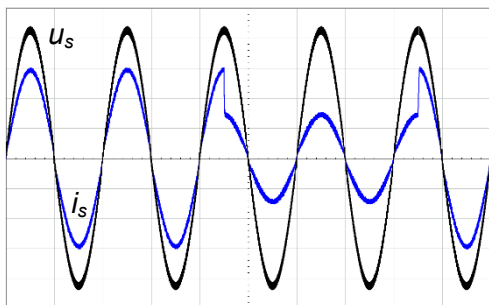


Fig.6. Waveforms of voltage u_s (75 V/div) and current i_s (6 A/div) during load changes for $t=0\div 100\text{ms}$, (10 ms/div)

Reference load was changed twice – from maximum power to half of the maximum, and to maximum again, during positive half period of the voltage at the connection point. For these two changes, the control system corrected waveform of the line current to reference in the same half period of voltage when the change took place.

In the next step, the operation of the converter was analyzed when the resonant frequency of the P+R controller was different from the grid frequency (50 Hz). The reference value of the line current corresponds to the maximum power that can be obtained from energy source, for the entire duration of the test. Waveforms of voltage and current when grid frequency (f_s) is different from controller resonant frequency (f_r) were shown in the figure 7÷8. In both cases (when $f_r < f_s$ – fig. 7 and $f_r > f_s$ – fig. 8), voltage and current waveforms are in phase with each other. Detuned controller at this level has no negative effect on the device operation.

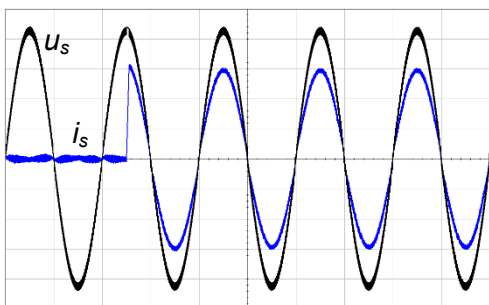


Fig.7. Waveforms of voltage u_s (75 V/div) and current i_s (6 A/div) for resonant frequency of the controller equal to 48 Hz for $t=0\div 100\text{ms}$, (10 ms/div)

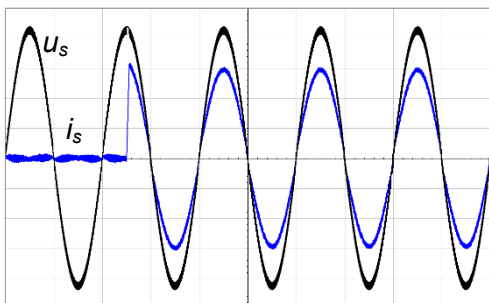


Fig.8. Waveforms of voltage u_s (75 V/div) and current i_s (6 A/div) for resonant frequency of the controller equal to 52 Hz for $t=0\div 100\text{ ms}$, (10 ms/div)

During the operation in conditions of deformation of the supply voltage (1st, 3rd, 5th, 7th harmonic included) in this way of generation of the reference signal, for one phase converter, voltage distortion had small influence on current deformation if current pattern was generated properly.

Current (with high frequency components and resistance of the line and choke omitted) has waveform as result of the equation (11):

$$(11) \quad i_s = L \frac{du_L}{dt} = L \frac{d(u_F - u_s)}{dt}$$

If:

$$(12) \quad u_F = u_S + u_{P+R}$$

So:

$$(13) \quad i_s = L \frac{du_L}{dt} = L \frac{d(u_F - u_s)}{dt} = L \frac{du_{P+R}}{dt}$$

Because of voltage deformation, current waveform pattern obtained in that way is also distorted. For that reason signal designed for current waveform pattern should be filtered or obtained by phase locked loop (PLL).

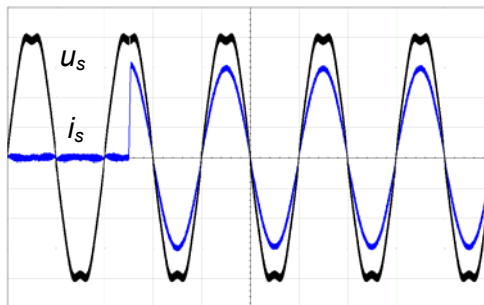


Fig. 9. . Waveforms of voltage u_s (75 V/div) and current i_s (6 A/div) in case of voltage distortion for $t=0\div 100\text{ms}$, (10 ms/div)

In table 1 ratios between 1st and other harmonics of the voltage and current were presented. Harmonics, which were added to voltage waveform had much smaller values in current waveform.

Table 1. Voltage and current harmonics

Harmonic	Ratio h/1h of the voltage [%]	Ratio h/1h of the current [%]
3	4.55	0.65
5	3.07	0.039
7	1.52	0.03

In figure 12, the reaction of the analyzed device in case of modulated changes of the voltage phase was presented. The voltage waveform with modulated phase can be described by equation:

$$(14) \quad u_s = U_m \sin(\omega t + \varphi(t))$$

where $\varphi(t)$ is modulating function. The phase of the voltage changed in range of $0\div 30^\circ$ with 5 Hz frequency (f_m) in time from $t=0$ to $t=0.2$ s. Waveform of the modulating function can be described by equation (15).

$$(14) \quad \varphi(t) = \frac{\Pi}{6} \sin(2\Pi f_m t)$$

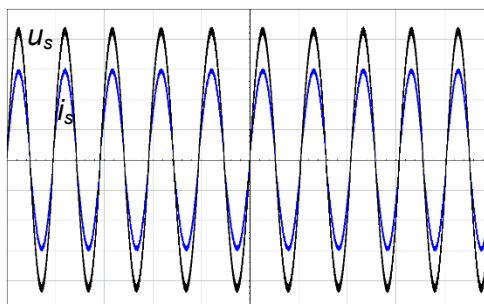


Fig. 10. Waveforms of voltage u_s (75 V/div) and current i_s (6 A/div) during phase modulation for $t=0\div 200\text{ms}$, (20 ms/div)

In the whole range of this changes, current waveform was in phase with voltage at the device point of connection with grid (fig. 11).

In order to study how the device will operate during voltage amplitude changes, system was supplied by modulated AC voltage source. The amplitude changed in the range of $0,85 \div 1,15U_N$ with 5 Hz frequency in time from $t=0.1$ to $t=0.3$ s. The voltage and current waveforms in that case were presented in fig. 11.

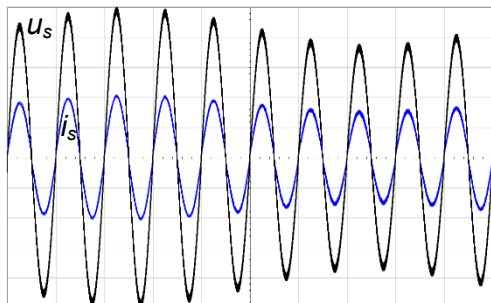


Fig.11. Waveforms of voltage u_s (75 V/div) and current i_s (10 A/div) for amplitude modulation for $t=100 \div 300$ ms, (20 ms/div)

When the amplitude of the voltage increased, the line current also increased and in the opposite situation when amplitude of the voltage decreased the line current decreased too. Current waveform is based on signal proportional (with fixed coefficient) to supply voltage so any changes of voltage waveforms causing changes in current waveform. Because of these voltage and current fluctuations, power obtained from energy source changes, too. This situation is unfavorable. Obtained power should be controlled on source side (in DC circuit) with, for example, PI controller. Then $k_{I|sRef}$ signal would be corrected so that the power level stays the same.

Summary

In the article, the results of the simulation studies of the proportional resonant controller P+R, obtained with P and I components, were presented. The Controller transmittance was formulated, synthesis was done, and finally the simulation model of 1 phase converter that connects power grid with energy source was elaborated. P+R controller can be used as a current controller in such applications. The Simulation studies also included typical states of power grid. During modulated changes of voltage phase which supply the converter, current was in phase with voltage for all the range of given changes. In case of voltage amplitude modulation, the current pattern of the supply line was also changing— therefore, the current drawn from the DC voltage source was also changing. The current on DC side should be controlled too, in order to preserve the power drawn from energy source.

Authors: Marek Nowak, MSc, Eng., Rzeszow University of Technology, Faculty of Electrical and Computer Engineering, W. Pola 2, 35-959 Rzeszów, E-mail: mnowak@prz.edu.pl; Prof. Stanisław Piórog, PhD, Eng., Rzeszow University of Technology, Faculty of Electrical and Computer Engineering, W. Pola 2, 35-959 Rzeszów, E-mail: pirog@prz.edu.pl.

REFERENCES

- [1] Sikorski A., Korzeniowski M., Malinowski M., „Przełącznik AC/DC/AC w małej elektrowni wodnej”, Przegląd Elektrotechniczny nr 6 (2011), s. 97.
- [2] Grodzki R., Sikorski A., Jasiński M., „Predykcyjne algorytmy sterowania trójfazowym przełącznikiem AC/DC”, Przegląd Elektrotechniczny nr 6 (2011), s. 105.
- [3] R. Teodorescu, F. Blaabjerg, M. Liserre, P.C. Loh, "Proportional-resonant controllers and filters for grid-connected voltage-source converters", IEE proceedings-Electric Power Applications, vol. 153, no. 5, pp. 750-762, Sep. 2006.
- [4] C. Hanju, V. Trung-Kien, K. Jae-Eon, "Design and control of Proportional-Resonant controller based Photovoltaic power conditioning system", Energy Conversion Congress and Exposition 2009. ECCE 2009, pp. 2198-2205.
- [5] A. Chatterjee, K. B. Mohanty, "Design and analysis of stationary frame PR current controller for performance improvement of grid tied PV inverters", 2014 IEEE 6th India International Conference on Power Electronics (IICPE), pp. 1-6, 2014.
- [6] D. Stojić, M. Milinković, S. Veinović and I. Klasnić, "Novel proportional-integral-resonant current controller for three phase PWM converters," 2016 4th International Symposium on Environmental Friendly Energies and Applications (EFEA), Belgrade, 2016, pp. 1-4.
- [7] T. Ngo, S. Santoso, "Improving proportional-resonant controller for unbalanced voltage and frequency variation grid," 2016 IEEE/PES Transmission and Distribution Conference and Exposition, May 2016, pp. 1-5.
- [8] O. Hemakesavulu, N. Chellammal, S. S. Dash, S. Lalitha, "A new PR-D (Proportional Resonant and Derivative) controller for resonance damping in a grid connected reverse voltage topology multi-level inverter," 2017 IEEE 6th International Conference on Renewable Energy Research and Applications (ICRERA), San Diego, CA, 2017, pp. 653-658.
- [9] H. Khalfalla, S. Ethni, M. Al-Greer, V. Pickert, M. Armstrong, V. T. Phan, "An adaptive proportional resonant controller for single phase PV grid connected inverter based on band-pass filter technique," 2017 11th IEEE International Conference on Compatibility, Power Electronics and Power Engineering (CPE-POWERENG), Cadiz, 2017, pp. 436-441.
- [10] M. Liserre, R. Teodorescu and F. Blaabjerg, "Multiple harmonics control for three-phase grid converter systems with the use of PI-RES current controller in a rotating frame," in IEEE Transactions on Power Electronics, vol. 21, no. 3, pp. 836-841, May 2006.
- [11] D. Stojić, M. Milinković, S. Veinović and I. Klasnić, "Novel proportional-integral-resonant current controller for three phase PWM converters," 2016 4th International Symposium on Environmental Friendly Energies and Applications (EFEA), Belgrade, 2016, pp. 1-4.
- [12] J. Zhang, L. Li, D. G. Dorrell and Y. Guo, "Space vector modulation based proportional resonant current controller with selective harmonics compensation for matrix converter systems," 2017 20th International Conference on Electrical Machines and Systems (ICEMS), Sydney, NSW, 2017, pp. 1-6.
- [13] M. Tariq, M. T. Iqbal, M. Meraj, A. Iqbal, A. I. Maswood and C. Bharatiraja, "Design of a proportional resonant controller for packed U cell 5 level inverter for grid-connected applications," 2016 IEEE International Conference on Power Electronics, Drives and Energy Systems (PEDES), Trivandrum, 2016, pp. 1-6.